Structural and compositional changes in the upper atmosphere related to the PEDE-2018 dust event on Mars as observed by MAVEN NGIMS

M. K. Elrod[1,2], S. W. Bougher[3], K. Roeten[3], R. Sharrar[3], J. Murphy[4]

[1]University of Maryland College Park, College Park, MD, USA.

[2]NASA Goddard Space Flight Center, Greenbelt, MD, USA.

[3]University of Michigan, Ann Arbor, MI, USA.

[4]New Mexico State University, Las Cruces, NM, USA.

Corresponding Author: Meredith Elrod (Meredith.k.elrod@nasa.gov)

Key Points:

- MAVEN/NGIMS observed increased of CO_2 and Ar densities observed in the upper atmosphere (160 – 250 km) corresponding to the peak of the dust event.
- Unexpected decrease in O densities in the upper atmosphere (160 – 250 km) was simultaneously observed.
- Comparisons between model and data results show good agreement with scale height and temperatures, further M-GITM model revisions needed to capture circulation effects.

This is the author manuscript accepted for publication and has undergone full peer review but has not been through the copyediting, typesetting, pagination and proofreading process, which may lead to differences between this version and the Version of Record. Please cite this article as doi: 10.1029/2019GL084378

Abstract

The onset of the Planet Encircling Dust Event (PEDE-2018) started around 1 June 2018 as observed by MRO/MARCI, peaking around 7-10 July, and persisting through mid-October 2018. After the onset of the event the upper atmosphere underwent significant changes in density and thermal structures. MAVEN NGIMS had a good opportunity to observe these changes from the first detection in the upper atmosphere and throughout the duration of the PEDE. The compositional changes included increased density at a constant altitude for CO_2 and Ar while the O decreased from the peak throughout the decay of the bulk of the PEDE.

Plain Language Summary

From June through October 2018 Mars experienced a Planet Encircling Dust Event (PEDE-2018), a fairly rare event last observed in 2007. The dust storm grew from a local event to cover the entire planet and was opaque enough that so that little sunlight reached the surface that the solar-powered Opportunity rover ceased operations and all attempts to re-establish contact with it were unsuccessful. Meanwhile, the orbiter MAVEN was able to observe changes in the upper atmosphere in the composition as a result of this globally extensive PEDE. MAVEN observed increases in both the CO_2 and Ar while also observing an unexpected reduction in the O densities.

1 Introduction

The recent Planet Encircling Dust Event (PEDE-2018) started around 1 June 2018, as viewed in context imaging from the MRO/Mars Color Imager (MARCI) [*Cantor et al.*, This issue]. The dust storm peaked around 7 – 10 July when the horizontal redistribution of dust around the planet was maximized, resulting in substantial warming of middle atmosphere (~25-

80 km) temperatures increasing atmospheric densities as determined by remote sensing data from the MRO/Mars Climate Sounder (MCS) [*Kass et al.,* This issue]. The progression of the storm is outlined in Table 1, which maps the significant events of the storm to date, Ls, latitude, and local solar time (TLST). These events are used as markers for the data and the model. Corresponding upper atmosphere (~160-300 km) responses in neutral densities and temperatures were measured in-situ by the MAVEN/ Neutral Gas and Ion Mass Spectrometer (NGIMS) during the first detection in the upper atmosphere and peak period. Unlike MCS, which has the ability to monitor remotely the middle to upper atmosphere climate and produce derived profiles of atmospheric densities and temperatures below 90 km, NGIMS, as an in-situ mass spectrometer, directly measures the density and composition of the upper atmosphere routinely above 150 km, the MAVEN nominal periapsis. This is the first PEDE at Mars to be observed with both an in-situ mass spectrometer and the remote sensors like MCS in orbit that is able to paint a picture of the compositional and structural changes in the upper atmosphere.

NGIMS sampling was conducted from solar zenith angle (SZA) 50^{o} (dayside) to SZA 150^{o} (nightside) from mid-latitudes in the southern hemisphere (~27°S) to high latitudes in the northern hemisphere (~55°N) during this dust storm period (Ls ~ 184 to 270). NGIMS measured neutral composition of the major gas species (He, O, CO, N_2, Ar and CO_2) [*Mahaffy et al.*, 2015]. Thermospheric scale heights and temperatures were derived from neutral density vertical structure using a fit method of the log (density) vs altitude as described in the Software Interface Specification (SIS) for the level 3 scale height product [*Benna and Elrod,* 2019]. This study focuses on the temporal variations in the NGIMS density and scale height for Ar, CO_2 and O during this PEDE event.

Previous observations have shown that the lower and middle atmosphere, specifically the CO_2 atmosphere, are heated by the influx of radiatively active dust into the atmosphere during dust events [Heavens et al., 2014, 2011, and references therein]. The MAVEN Accelerometer (ACC) is able to give a picture of the thermospheric mass density responses during the PEDE dust storm [*Zurek et al.*, 2018], while NGIMS provides the density and temperature variations of the Ar, CO_2, and O, from ~160 – 200 km. Consistent with the thermodynamic characterizations of the middle atmosphere observations from MCS and the higher altitude ACC data that observed an increase in the total neutral densities, NGIMS also observed substantial enhancement in Ar and CO_2 densities corresponding with the peak of the dust event. However, different and unexpected from these observations, NGIMS observed a reduction in atomic O densities during the peak of the PEDE.

The new observation of reduction of O during the PEDE indicates that there are a number of dynamical effects going on during the dust events that will change and improve thermospheric modeling simulations like those conducted using The Mars Global Ionosphere-Thermosphere Model (M-GITM) [*Bougher et al*., 2015]. NGIMS wind data measurements taken during the first detection in the upper atmosphere and peak of the PEDE and monthly throughout the mission are helping to constrain the M-GITM model [*Roeten et al.,* 2019, *Benna et al.,* 2019]. These models are working on compensating for the modified circulation during the dust storm. This oxygen reduction may also be partially linked to photochemistry beyond the modified thermospheric circulation dynamics.

2 Methods and Data

MAVEN NGIMS is a quadropole mass spectrometer capable of measuring neutral and ion species from mass 1.5 – 150 Da in 0.1 increments. It is capable of creating accurate profiles

of the neutral atmosphere from periapsis (~150 – 160km for nominal science operations, ~125km for deep dip or aerobraking campaigns) to ~300km for major atmospheric species (Ar, CO_2, N_2, CO, O, and He). Regular science orbits switch between neutral and ion modes of observation throughout the orbit allowing for nearly simultaneous measurements of ion and neutral densities from ~400km to periapsis at ~150km for ion masses 2 – 60 in 1 Da increments. At the beginning of the PEDE, NGIMS conducted two 10 orbit wind campaigns, which does not produce regular neutral density data, these are not included. With emphasis on the Ar, CO_2, and O abundances, the neutral density data used in this study were obtained from the MAVEN NGIMS level 2 (csn-abund) data products version 8 revision 1, and the scale heights were obtained from the NGIMS level 3 (res-sht) data products version 6 revision 1. All MAVEN NGIMS data products are available on the Planetary Data System (PDS).

In order to track the changes in the atmosphere during the dust event, we examined the NGIMS-provided inbound neutral Ar, CO_2, and O density at a constant altitude of 170 km before, during, and after the PEDE (Fig. 1a). Figure 1a plots the Ar (blue), CO_2 (red) and O (black), with abundances in particles/cc, from just prior to the onset and peak of the PEDE through the decay phase of the dust storm as the atmosphere began to reach equilibrium again. The solid lines represent 10-orbit averages throughout the data. The thick vertical purple line indicates the first upper atmosphere detection of the PEDE, and the thick vertical green line indicates the start of the decay phase of the PEDE. The black dashed line marks the SZA for this time period for reference. Figure 1b is a zoomed in view of figure 1a and focuses on just the first detection in the upper atmosphere and peak of the dust event in order to showcase the enhancement of the Ar and CO_2 while the O is decreasing over the same interval. The MAVEN observations were made from dayside (SZA $<85^o$) to nightside SZA $>105^o$) from the beginning

of the PEDE to the end of the PEDE and from mid southern latitudes to high northern latitudes (at 170 km).

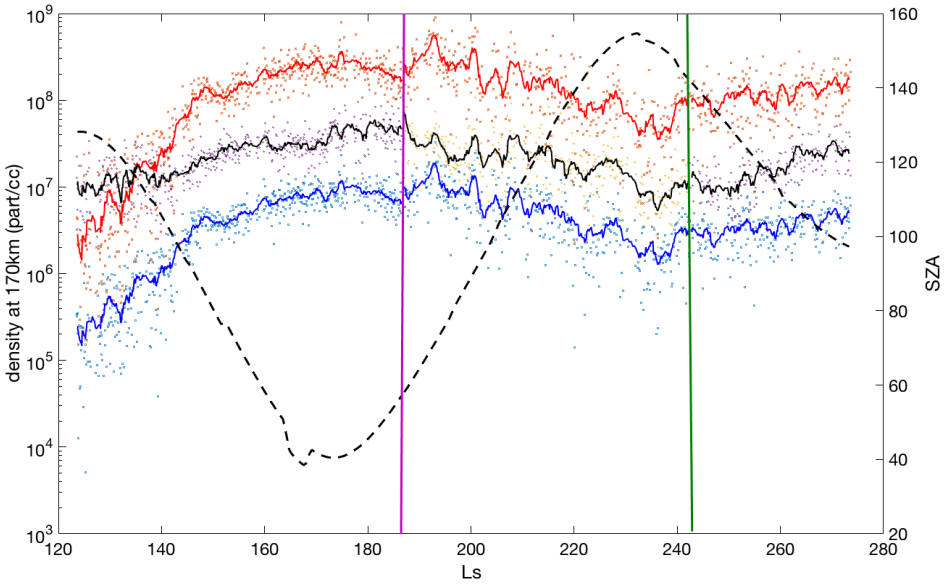

(a)

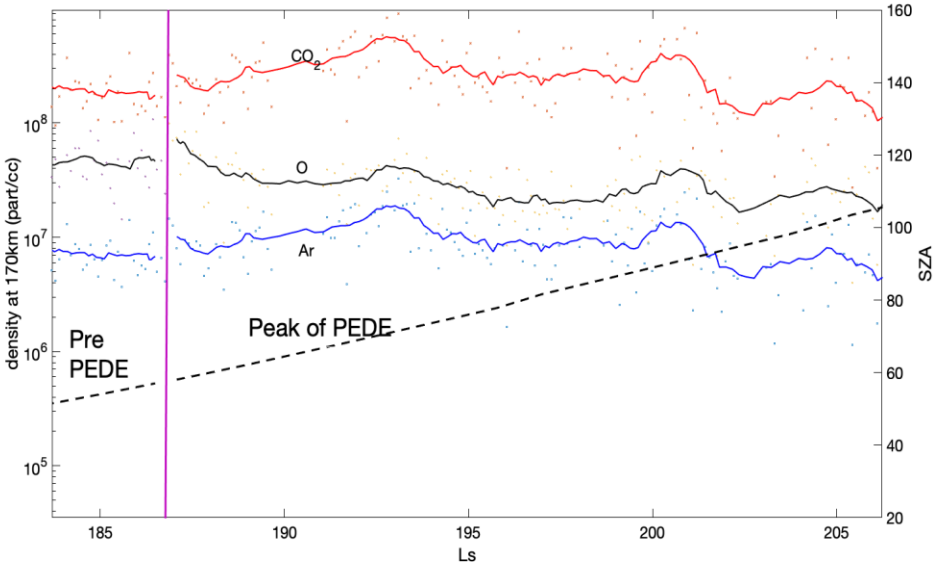

(b)

Fig 1: (a) CO_2 (red line), Ar (blue line), O (black solid line) densities (cm^{-3}) at 170km the dark lines are a 10-orbit average and the dots are the individual orbits indicating the orbit

to orbit scatter. The solid vertical purple line marks the first upper atmosphere detection of the PEDE, the solid vertical green line marks the start of the decay phase of the PEDE. The black dashed line is the observed SZA for MAVEN NGIMS. (b) A zoomed-in segment of (a) that highlights just the first detection in the upper atmosphere through the peak and start of the decay period of the PEDE. Using this enlargement of 1a it is easier to see the enhancement of CO_2 and Ar while the O is decreasing at the same time highlighting the decoupling of these species during the dust storm.

In order to determine how much of a change occurred as a result of the PEDE we divided the NGIMS data into a pre-PEDE section from MY 33 and MY 34 prior to the dust storm and cutting off before the smaller regional dust storms in MY 33 and data from the PEDE. This allows the pre-PEDE data to contain nominal Mars atmospheric data over most latitudes, solar zenith angles (SZA), and longitudes. We then divided the data from the PEDE into two sections of data: 1) from the first upper atmosphere detection through the start of the decay phase (on figure 1a between purple and green lines) (PEDE data), and 2) from the start of the decay phase through mid-decay (Ls 240 – 250) (decay data). Finally, a section was defined for the post decay through end 2018 (post-PEDE). These sections of data were each first binned at a constant altitude of 170 km then binned by SZA from 0 to 150 degrees in 10-degree bins. We chose 170 km since it is high enough above periapsis to reduce the horizontal observational errors, and low enough that data is above the background for all species. We then computed the ratio of PEDE to pre-PEDE by SZA at 170 km. Figure 2a plots the ratio between the PEDE and pre-PEDE densities for Ar (blue), CO_2 (red) and O (purple). In this figure if the ratio is >1 the abundances experienced an increase during the PEDE and if the ratio is <1 then the atmosphere or species experienced reduction during the PEDE. Figure 2a indicates that Ar and CO_2 densities increased

significantly, by about a factor of 5, on the nightside (SZA >110^{o}). Additionally, we collected all the NGIMS inbound neutral density data from the pre-PEDE and the PEDE data and binned these measurements by $\log_{10}(\text{dens}CO_2)$ from 3 to 14 in 0.1 steps. This allows for examination of all data over all sampling altitudes and SZA. By continuing to divide this between PEDE and pre-PEDE periods, this allows us to examine how much the Ar and CO_2 increased vs the total (Ar + CO_2 + O) atmosphere and how O decreased. Figure 2b plots the density of Ar (red-PEDE magenta pre-PEDE) CO_2 (black-PEDE, yellow-pre-PEDE) and oxygen (blue-PEDE cyan pre-PEDE). Atomic O underwent a decrease in the densities during the event of approximately 20% during both day and nightside. Figure 2 a&b demonstrate that while Ar and CO_2 track well together, O not only was more affected by the global circulation during the PEDE but also saw a significant decrease during the PEDE.

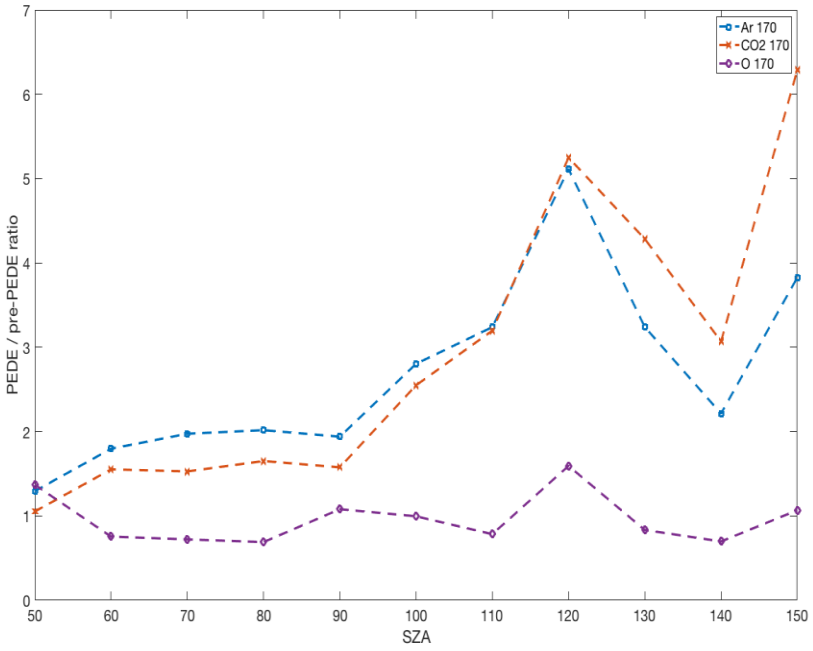

(a)

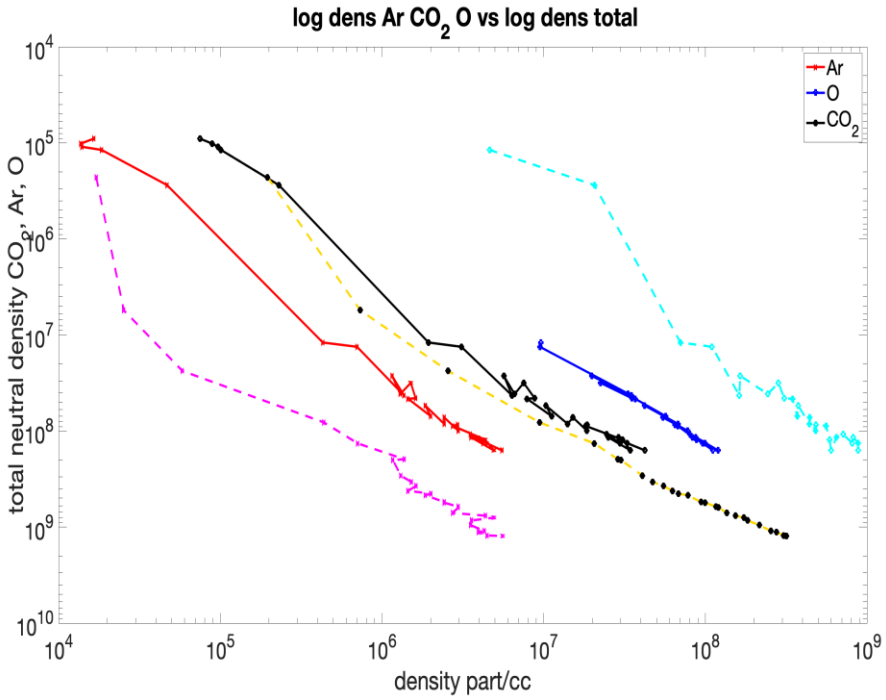

(b)

Fig 2: (a)CO_2 (red x's), Ar (blue squares), O (purple diamonds), ratio of PEDE to pre-PEDE density (part/cc) at ~170km versus SZA. A ratio of 1 would indicate no change between the peak of the PEDE and the average density, > 1 indicates the density increased during the dust event, and < 1 indicates decrease during the PEDE. (b) Plot of Ar (red PEDE and magenta pre-PEDE) CO_2 (black PEDE and yellow pre-PEDE) and O (blue PEDE and cyan pre-PEDE) data binned by $\log_{10}$ dens(CO_2) from 3 to 12 by 0.1 steps. (Dashed curves are all pre-PEDE, solid curves are PEDE)

3 Model comparison and Discussion

NGIMS has ram pointing on the MAVEN spacecraft, the orbital geometry transitioned from the dayside to the nightside of the planet during the PEDE-2018 event. The time-evolving dust storm as well as latitude/local time sampling biases are convolved in MAVEN observations and disentangling these drivers requires the use of 3-D Global Circulation Model (GCM). The

Mars Global Ionosphere-Thermosphere Model (M-GITM) is utilized to simulate thermospheric impacts during this dust event, thereby incorporating both of these drivers. [e.g. *Bougher et al.,* 2018].

The M-GITM code is a 3-D spherical model that was developed to address the physics of the entire Mars atmosphere system, capturing the basic observed features of the dynamical, thermal, and composition of the atmosphere from ground to ~250 km [*Bougher et al.*, 2015]. The M-GITM framework was built from the terrestrial GITM framework [*Ridley et al.*, 2006], now including Mars fundamental physical parameters, ion-neutral chemistry, and key radiative processes [*Bougher et al.*, 2015]. Typically, the model is setup to run with a 5°x 5° latitude-longitude grid, and a 2.5 km resolution.

This ground to exosphere code is built upon existing parameterizations and physical formulations found in other modern GCMs (see details in *Bougher et al*., 2015). Features important for this PEDE study are briefly outlined. For the Mars lower atmosphere (0-80 km), dust opacity distributions can be prescribed based upon empirical dust opacity maps obtained from several Martian years of measurements [e.g. *Smith,* 2004, 2009; *Montabone et al.*, 2015]. For the Mars upper atmosphere (~80 to 250 km), a fast and modern formulation for non-LTE CO_2 15-micron cooling was recently implemented within the M-GITM code [e.g. *Gonzalez-Galindo et al.,* 2013] to accurately capture the CO_2 cooling rates [e.g. *Bougher et al*., 2018].

Further upgrades to the M-GITM code were implemented to permit accurate solar irradiance and dust opacity inputs to be utilized for the PEDE simulations. First, the solar EUV-UV fluxes measured at Mars by the MAVEN Extreme Ultraviolet Monitor (EUVM) instrument have been used to assemble the FISM-M (Flare Irradiance Spectral Model – Mars) empirical model, yielding daily averaged full solar spectra [*Thiemann et al.*, 2017]. These daily averaged

datasets provide solar EUV-UV fluxes to M-GITM corresponding to MAVEN-specific orbit measurements. Second, model inputs for time varying dust integrated optical depths and vertical dust distributions during the PEDE are utilized. The latter is based upon MRO/MCS dust opacity datasets (V.5.2.7) [e.g *Heavens et al.,* 2014; *Kass et al.*, this issue] as a function of derived pressure intervals (103) and zonally averaged latitude elements (36) to match the M-GITM horizontal resolution. The 3-D dust distribution fields possessing zonally uniform but vertical and latitude structure are used to calculate aerosol heating rates within the M-GITM code. These 3-D maps are derived from MCS opacity datasets for 9-reference time intervals (Table 1) corresponding to major milestones during the PEDE evolution. Linear interpolation in time between these reference intervals is conducted, yielding vertical and latitudinal (and zonally uniform) dust distributions for use by the M-GITM code throughout each simulated day. Future updates to this M-GITM formulation will relax these assumptions and make use of updated MCS datasets (V5.3) for this PEDE period.

Densities (CO_2, Ar, and O), scale heights, and temperatures corresponding to NGIMS thermospheric measurements are extracted from the M-GITM output data-cubes throughout this simulated PEDE evolution. Extraction requires the use of NGIMS trajectory files for each orbit, detailing the latitude, longitude, local time and altitude coordinates of measurements conducted along the orbit path below ~250 km. A M-GITM flythrough routine is utilized for this extraction at each actual measurement location, yielding the corresponding M-GITM densities, temperatures, and scale heights at the same location and time.

Figures 3 a & b show comparisons between the NGIMS data and the results from the M-GITM modeling from the PEDE peak period (Ls ~185 – 240). Figure 3a compares the Ar (NGIMS red, M-GITM magenta) and CO_2 (NGIMS blue, M-GITM cyan) scale heights (top

panel) from NGIMS data to corresponding M-GITM values. 10-orbit averaged (orbit range 7143 – 7640) and corresponding 1-σ error bars are presented for these NGIMS scale heights. Scale heights from NGIMS data are determined by log(density) vs altitude linear fits. The NGIMS temperatures plotted in the bottom panel of Figure 3a are derived from the Ar scale heights using T = mgH/k where m is mass, g is gravitation, H is scale height and k is Boltzmann constant since Ar is the non-reactive species and best for temperature measurements [*Benna and Elrod,* 2019]. However, since M-GITM is primarily a climate model that includes solar fluxes on a daily cadence, it does not reproduce well the high orbit-to-orbit variability observed by NGIMS during the PEDE.

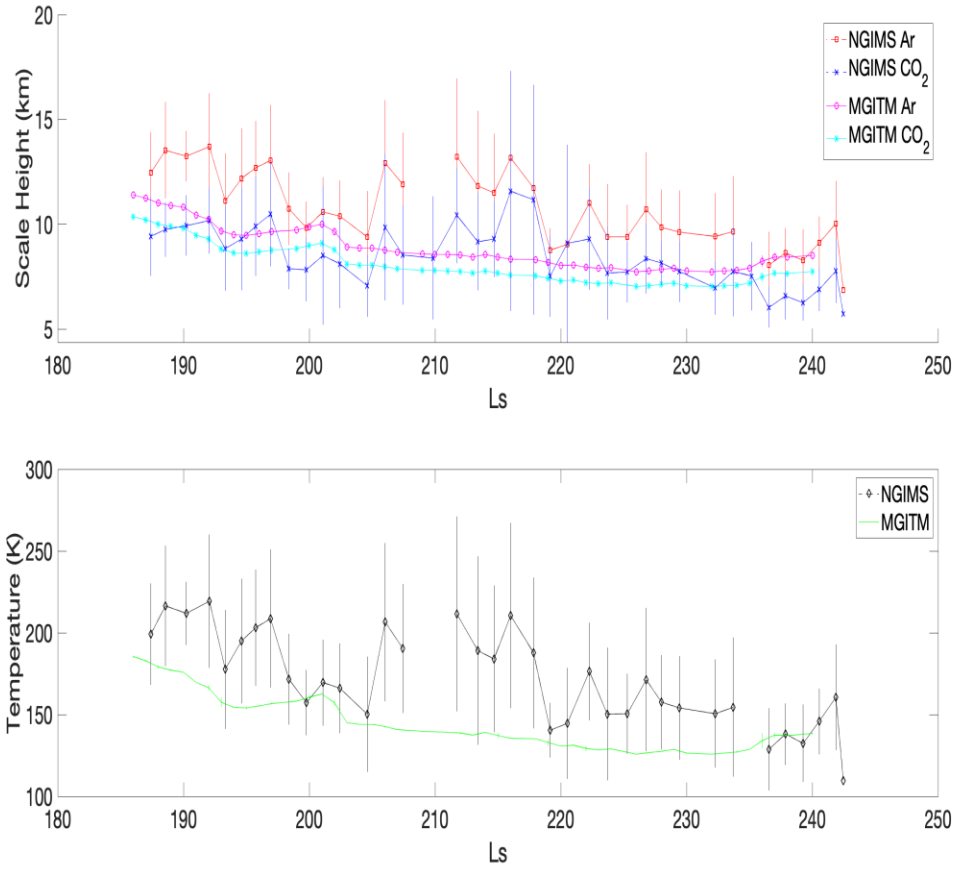

(a)

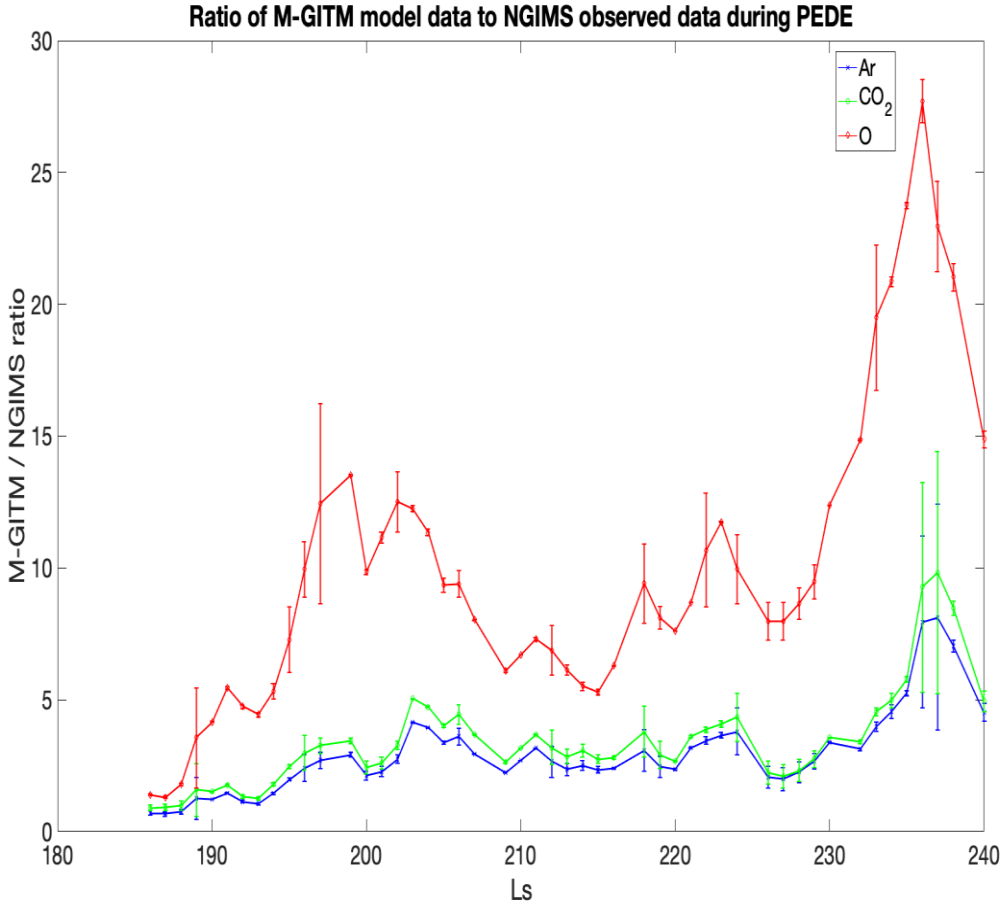

(b)

Figure 3(a): NGIMS scale height (km) of CO_2 (red), Ar (blue), and M-GITM Ar (magenta) and CO_2 (cyan) scale heights vs Ls, for the peak of the dust event (top panel). Temperature (K) for NGIMS (black) and M-GITM (green) (bottom panel). Vertical bars are 1-σ error bars of the orbit-to-orbit variability. (b) Ratio of M-GITM model densities to NGIMS densities from the PEDE dust first upper atmosphere detection and peak period. Ar (blue) CO_2 (green) and O (red).

In comparing the densities between the model and the NGIMS data, however, the hydrostatic expansion of the heated lower-to-middle atmosphere during the PEDE plus the simulated thermospheric circulation created a substantial difference in the results. Figure 3b plots

the ratio of M-GITM to NGIMS for Ar, CO2 and O densities during the first upper atmosphere detection and peak of the PEDE. A ratio of 1 would indicate that these values agree, <1 would indicate that the model underestimates the observed densities and >1 the model overestimates the observed densities. Ar (blue) and CO_2 (green) trend higher by a factor of ~3-5 throughout the PEDE, while O (red) is overestimated by a larger factor of ~10-20 throughout the PEDE. This indicates the model is not warming the lower and middle atmosphere enough or that the circulation has changed. The NGIMS scale heights appear to be somewhat higher during the PEDE which suggests downwelling motion and adiabatic warming along the MAVEN periapsis track.

Simulated atomic O distributions are particularly subject to transport from day to nightside resulting in local bulges in the upper thermosphere near the evening terminator [e.g. *Bougher et al.,* 2015]. These bulges were not observed at the same locations in the NGIMS data during the PEDE peak period (fig 3b). These results indicate that the M-GITM model will need some further updates, including modifications of circulation, wind, and transport dynamics, to improve atomic oxygen densities throughout the PEDE.

The differences in the predicted model data densities provide a pathway for improvement of the modeling efforts thereby enhancing our understanding of how the thermospheric circulation is maintained impacted during dust events. The absence in the model of gravity wave momentum and energy deposition is likely a major contributor to the predawn data-model discrepancies, especially at high latitudes [*Zurek et al.,* 2017]. In addition, when the atmosphere is highly turbulent (variable) like it is on the night side or as it was during this PEDE dust event, obtaining good data-model agreement can be particularly difficult [*Zurek et al*., 2017]. The new

results from this PEDE dust storm will help improve detailed model investigations and dust storm period thermospheric circulation studies [e.g. *Bell et al.,* 2007; *Medvedev, et al.,* 2013].

In addition to the circulation and vertical transport mechanisms, there are other photochemical effects in the middle and upper atmosphere that could have an impact on the decrease in atomic oxygen during the PEDE. Oxygen is a highly volatile element and is reactive with ice, water, CO, CO2, OH, and all associated ions. During the PEDE water ice clouds were observed higher in the atmosphere (~80 km) [*Cantor et al.,* 2019]. It is possible that this ice formation is an atomic oxygen sink since the oxygen sticks to the ice. With the higher opacity in the atmosphere due to the dust the photodissociation from the ice is reduced keeping the oxygen on the ice until the tail end of the storm. Another possibility, though smaller effect, could be due to photoionization of the oxygen from top down. Ion data indicates that there was an increase in water group ions (H_2O^+, OH^+, H_3O^+). This is something to consider in future studies.

Table 1: Progression of the PEDE dust storm timeline based on MRO/MCS observations.

Date (2018)	**Ls (deg)**	***Periapsis Latitude (deg)**	***Periapsis TLST (hours)**	**Milestone**
June 1	185.2	27.0 S	8.8	Onset of storm
June 8	189.2	19.0 S	7.8	1st upper atmosphere detection
June 12	191.6	16.0S	7.4	Growth Phase

June 16	194.0	13.0S	7.1	Growth Phase
June 17	194.5	10.0 S	6.7	PEDE declared
June 27	200.4	5.0 S	6.0	MAVEN Periapsis to nightside
July 7-10	207-208	4.0 N	5.0	Peak of PEDE
August 15	230.5	27.0 N	2.0	Early Decay Phase
Sept 15	250.1	55.0N	21.7	Mid- Decay Phase

4 Summary & Conclusions

The PEDE dust event that began 1 June 2018 on Mars caused increases of the upper atmosphere (~150-270 km) CO_2 and Ar densities at a constant altitude as observed by MAVEN NGIMS instrument while simultaneously and unexpectedly decreasing the atomic O densities. Observations of PEDE dust storms made by MRO/MCS also observed an increase of the middle and upper CO_2 atmosphere temperatures (~80-120 km) [*Kass et al.*, this issue]. M-GITM modeling efforts to describe the thermospheric structure and circulation during the PEDE dust storm produced scale height, temperature and densities for comparison with NGIMS data. This comparison showed some agreement with the 170 km temperatures and scale heights within the 1-σ error of the NGIMS data while the later suggested somewarming, perhaps associated with downward motion and adiabatic warming. However, when comparing the M-GTIM density

results with the NGIMS measurements, the much higher computed densities at 170km suggest the hydrostatic expansion of the heated lower-to-middle atmosphere and the associated M-GITM thermospheric dynamics are in need of revision. The scale heights and temperatures respond to local effects making the M-GITM computed results and observed NGIMS results more consistent. However, CO_2 and Ar densities respond to the hydrostatically integrated atmosphere (and for atomic O local thermospheric transport) and are therefore subject to changes from below. Both of these effects combine to control thermospheric structure and dynamics during the PEDE and help to explain why the computed and observed densities are so different [*Thiemann et al.*, 2018].

The novel observations made during this PEDE dust event include the observations of the depletion of oxygen during the peak of the dust storm. The O was depleted by approximately 20% at the peak of the storm and returned to normal levels slowly throughout the decay of the storm. Future work will include examining the smaller regional dust storms that occurred in MY 33 and the secondary storms after this PEDE that occurred in the beginning of 2019 for a similar effect on the neutral O. This future work will also include examination of the ionosphere and possible photochemistry from the middle and lower atmosphere.

Acknowledgments, Samples, and Data

Special acknowledgments to the MAVEN NGIMS team at NASA Goddard SFC, and the MAVEN operations team at LASP and Lockheed Martin in Colorado. All data are archived in the Planetary Atmospheres Node of the Planetary Data System (http://pds.nasa.gov). Data through August 15, 2016 is available on the Planetary Data System (PDS4) (e.g. *mvn_ngi_l2_csn-abund-28754_20180829T124721_v08_r01.csv*.

mvn_ngi_l3_res-sht_28754_20180829T124721_v06_r01.csv)

These data are also available upon request. The authors thank the MRO MCS Team for making available MCS-derived profiles for creation of the dust opacity maps used in the MGITM simulations; those MCS data are now available within the NASA PDS. M-GITM outputs used for data-model comparisons are available on the Deep Blue Data (https://deepblue.lib.umich.edu/data) repository at the University of Michigan Library. The MAVEN mission has been funded by NASA through the Mars Exploration Program. This research is funded in part by the CRESST II cooperative agreement with NASA GSFC and University of Maryland College Park.

References

Bell, J. M., S. W. Bougher, and J. R. Murphy, Vertical dust mixing and the interannual variations in the Mars thermosphere, J. Geophys. Res., 112, E12002, doi:10/1029/2006JE002856, (2007).

Benna and Elrod, Mars Atmosphere and Volatiles Evolution (MAVEN) Mission Neutral Gas and Ion Mass Spectrometer (NGIMS) PDS Software Interface Specification (2019) pd.nasa.gov.

Benna, M., S. W. Bougher, Y. Lee, K. J. Roeten, E. Yigit, P. R. Mahaffy, and B. M. Jakosky, MAVEN reveals the global circulation of the upper-atmosphere of Mars, accepted, aax1553, (2019).

Bougher, S. W., D. A. Brain, J. L. Fox, F. Gonzalez-Galindo, C. Simon-Wedlund, and P. G. Withers. Chapter 14: Upper Atmosphere and Ionosphere, in The Atmosphere and Climate of Mars, ed. B. Haberle, M. Smith, T. Clancy, F. Forget, R. Zurek, Cambridge University Press, (2017), doi:10.1017/9781107016187.

Bougher, S. W., K. J. Roeten, M. Benna, P. R. Mahaffy, M. K. Elrod, and D. J. Pawlowski, The Responses of the Mars Thermosphere to the PEDE-2018a Dust Event: MAVEN NGIMS Measurements and Corresponding Global Model Simulations, AGU Fall 2018 Meeting, AGU Supplement #XXX, abstract P43J-3873, (2018).

Bougher, S. W., D. Pawlowski, J. Bell, S. Nelli, T. McDunn, J. Murphy, M. Chizek, and A. Ridley, Mars Global Ionosphere Thermosphere Model (M-GITM): I. Solar Cycle,

Seasonal, and Diurnal Variations of the Upper Atmosphere, JGR-Planets, 120, 311- 342, (2015). doi:10.1002/2014JE004715.

Cantor, B.A., Malin, M.C., 'MRO MARCI Observations of the Evolution of the 2018 Planet-Encircling Dust Event" AGU FM 2018, 2018AGUFM.P34A..01C

Haberle, R. M., J. L. Hollingsworth, A. Colaprete, A. F. C. Bridger, C. P. McKay, J. R. Murphy, J. Schaeffer, and R. Freedman , The NASA/AMES Mars General Circulation Model: Model improvements and comparison with observations, in Published Conference Abstract, International Workshop: Mars Atmosphere Modelling and Observations, (2003).

Heavens, N. G., M. I. Richardson, A. Kleinbo¨hl, D. M. Kass, D. J. McCleese, W. Abdou, J. L. Benson, J. T. Schofield, J. H. Shirley, and P. M. Wolkenberg, The vertical distribution of dust in the Martian atmosphere during northern spring and summer: Observations by the Mars Climate Sounder and analysis of zonal average vertical dust profiles, Journal of Geophysical Research: Planets, 116(E4), (2011). doi:10.1029/2010JE003691.

Heavens, N.G., Johnson, M.S., Abdou, W.A., Kass, D.M., Kleinb, A., McCleese, D.J., Shirley, J.H., and Wilson, R.J.: 2014, Seasonal and diurnal variability of detached dust layers in the tropical Martian atmosphere J.Geophys. Res. E 10.1002/2014JE004619

Gonzalez-Galindo, F., Chaufray, J-Y., López-Valverde, M.A., Gilli, G., Forget, F., Leblanc, F., Modolo, R., Hess, S., Yagi, M., "Three-dimensional Martian ionosphere model: I. The photochemical ionosphere below 180km" *J. Geophys, Res*., **118,** 2105-2123, (2013). 10.1002/jgre.20150

Kass, D.M., Kleinboehl, A., Shirley, J.H., Schofield, J.T., McCleese, D.J., Heavens, N.G., 'Mars Climate Sounder Observations during the 2018a Global Dust Event' AGU FM 2018 2018AGUFM.P43J3862K

Keating, G. M. et al., The Structure of the Upper Atmosphere of Mars: In-situ Accelerometer Measurements from Mars Global Surveyor, Science, 279, 1672-1676, (1998).

Mahaffy, P. R., M. Benna, M. Elrod, R. V. Yelle, S. W. Bougher, S. W. Stone, and B. M. Jakosky, Structure and Composition of the Neutral Upper Atmosphere of Mars from the MAVEN NGIMS Investigation, Geophys. Res. Lett., 42, 8951-8957, (2015). doi:10.1002/2015GL065329.

Medvedev, A. S., E. Yi˘git, T. Kuroda, and P. Hartogh (2013), General circulation modeling of the Martian upper atmosphere during global dust storms, J. Geophys. Res. Planets, 118, 2234–2246, doi:10.1002/2013JE004429.

Montabone, L., F. Forget, E. Millour, R. J. Wilson, S. R. Lewis, B. Cantor, D. Kass, A. Kleinbohl, M. T. Lemmon, M. D. Smith, M. J. Wolff, Eight-year climatology of dust

optical depth on Mars, Icarus, 251, 65-95, (2015). http://dx.doi.org/10.1016/j.icarus.2014.12.034.

Roeten K. J., S. W. Bougher, M. Benna, P. R. Mahaffy, Y. Lee, D. Pawlowski, F. Gonzalez-Galindo, M. A. Lopez-Valverde, MAVEN/NGIMS thermospheric neutral wind observations: Interpretation using the M-GITM general circulation model, J. Geophys. Res.- Planets, accepted, 2019JE005957, (2019)

Smith. M. D., Inter-annual variability in TES atmospheric observations of Mars during 1999-2003, **Icarus, 167**, 148-165 (2004).

Smith, M. D., THEMIS observations of Mars aerosol optical depth from 2002- 2008, Icarus, 202, 444–452, (2009). doi:10.1016/j.icarus.2009.03.027

Thiemann, E., P. C. Chamberlin, F. Eparvier, T. Woods, S. W. Bougher, B. M. Jakosky, and B. Templeman, The MAVEN EUVM spectral irradiance model for solar variability at Mars: Algorithms and results, J. Geophys. Res. Space Physics, 122, 2748-2767, (2017). doi:10.1002/2016JA023512.

Zurek, R. W. , D. Kass , S. W. Bougher, S. Demcak, R. Tolson, D. Baird, R. Lugo, B. Jakosky The 2018 Planet-Encircling Dust Storm: Effects on the Mars Upper Atmosphere as seen in MAVEN Navigation and Accelerometer Data. AGU Fall 2018 Meeting, AGU Supplement #XXX, abstract P43J-3864, (2018).

Zurek, R. W., R. H. Tolson, S. W. Bougher, D. Baird, R. Lugo, J. M. Bell, and B. M. Jakosky, Mars thermosphere as seen in MAVEN Accelerometer data, J. Geophys. Res. Space Physics, 122, 3798-3814, (2017). doi:10.1002/2016JA023641.

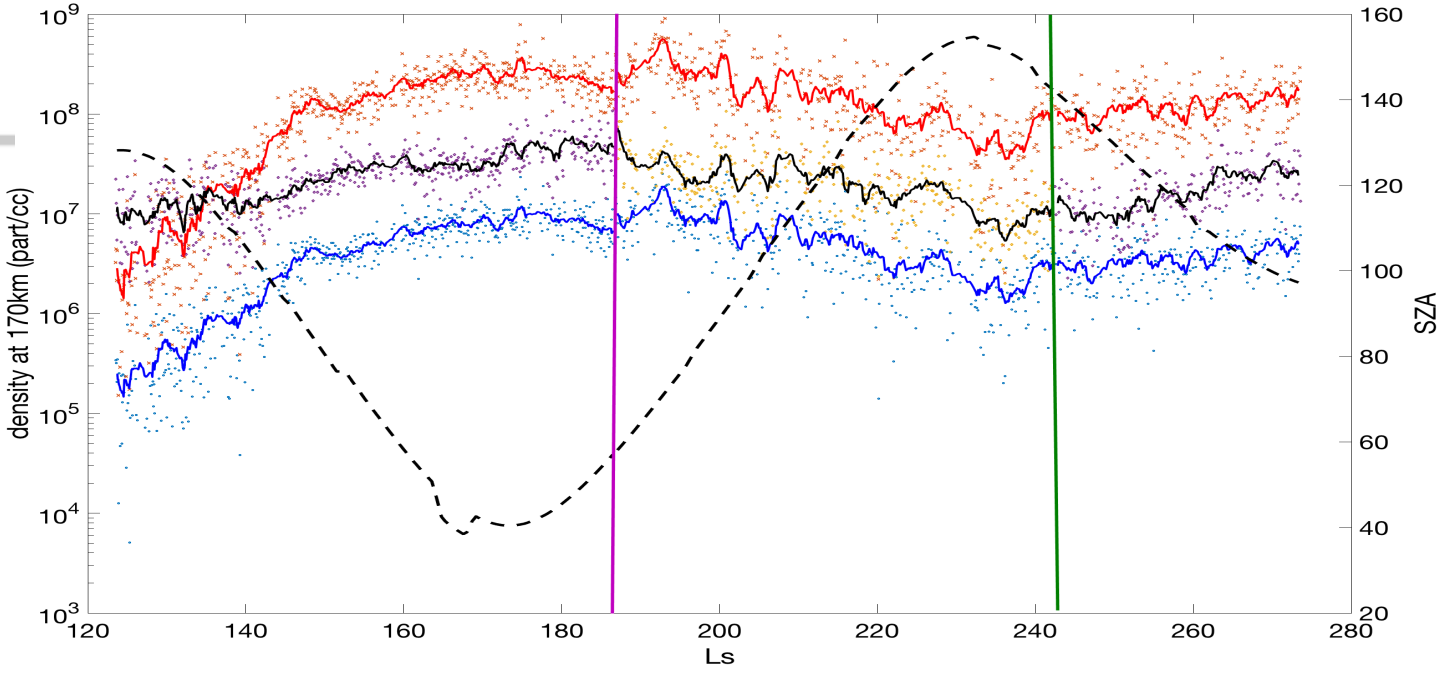

(a)

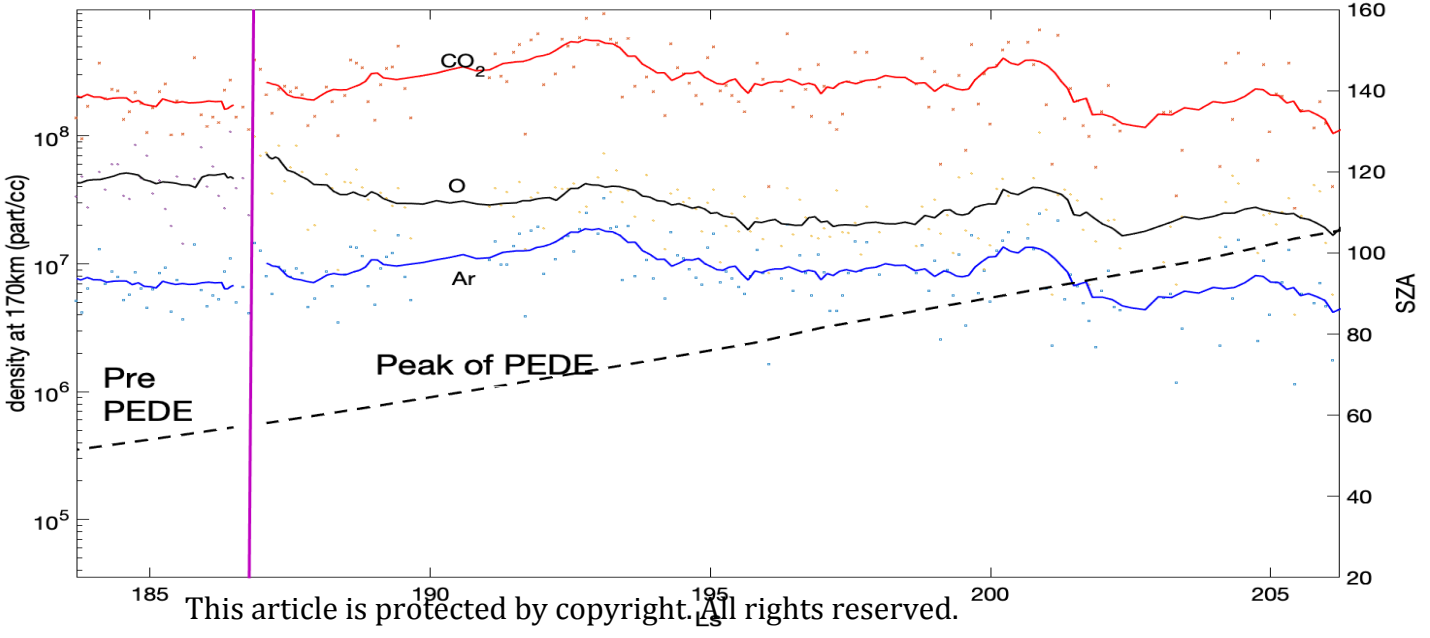

(b)

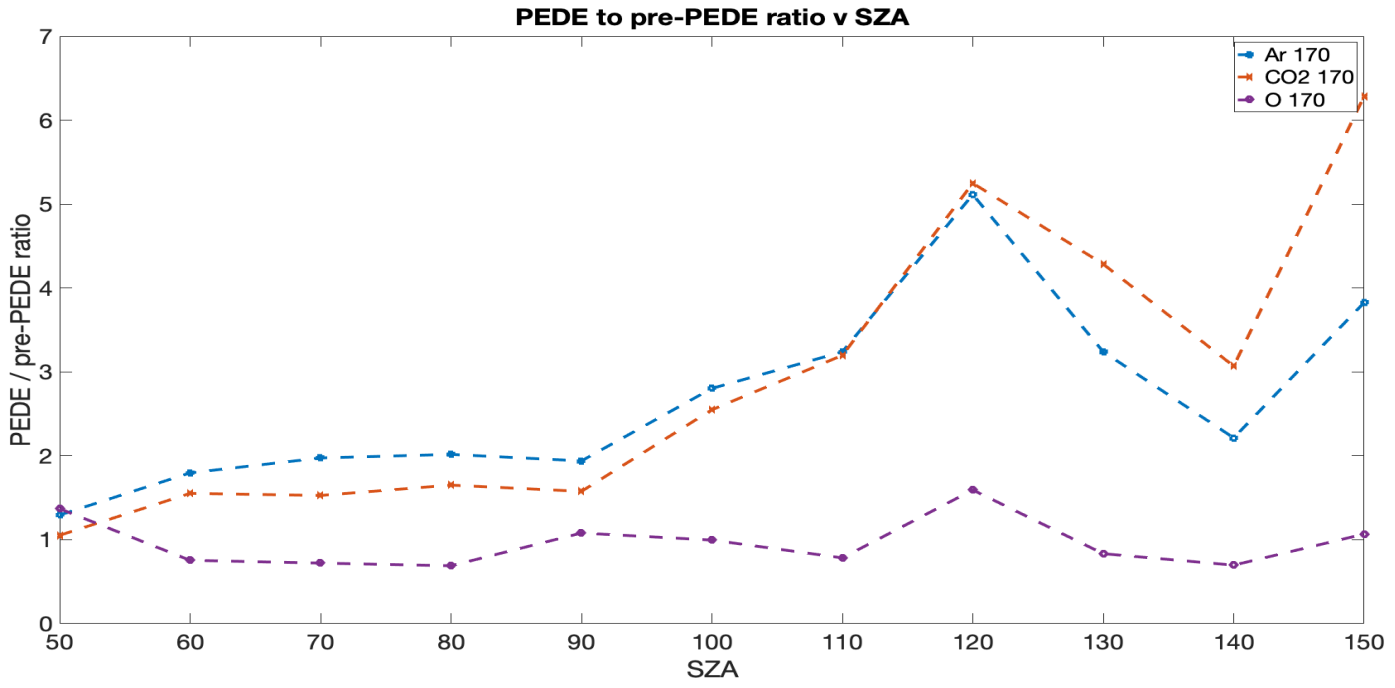

(a)

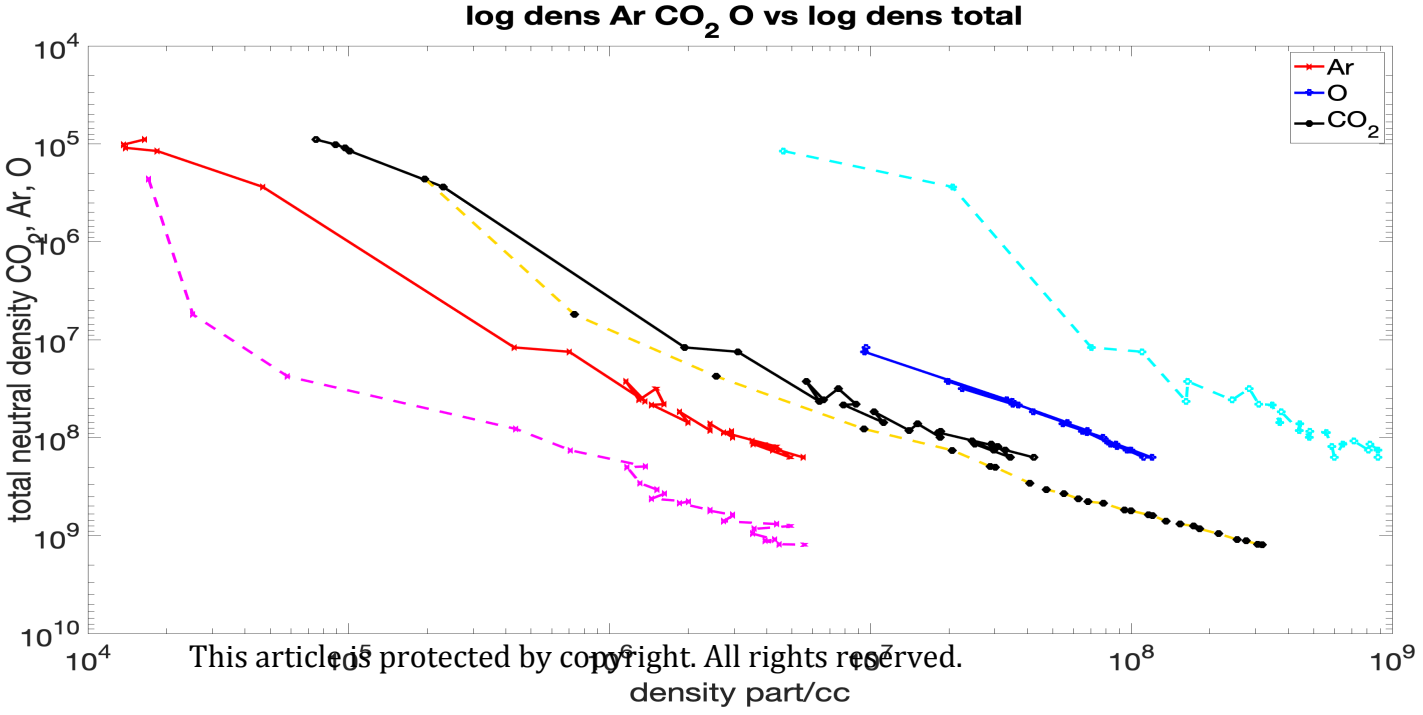

(b)

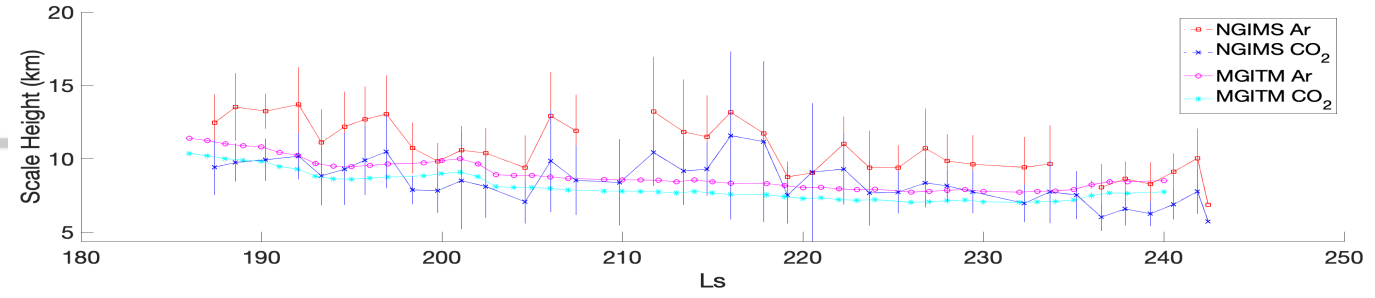

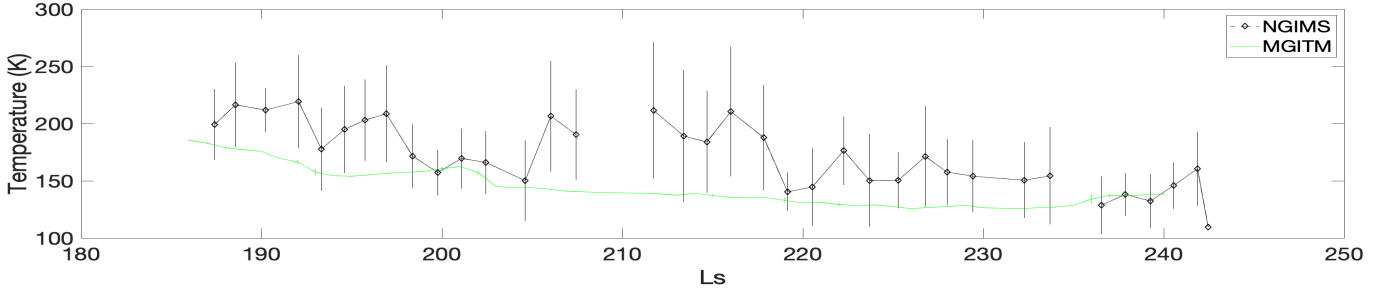

(a)

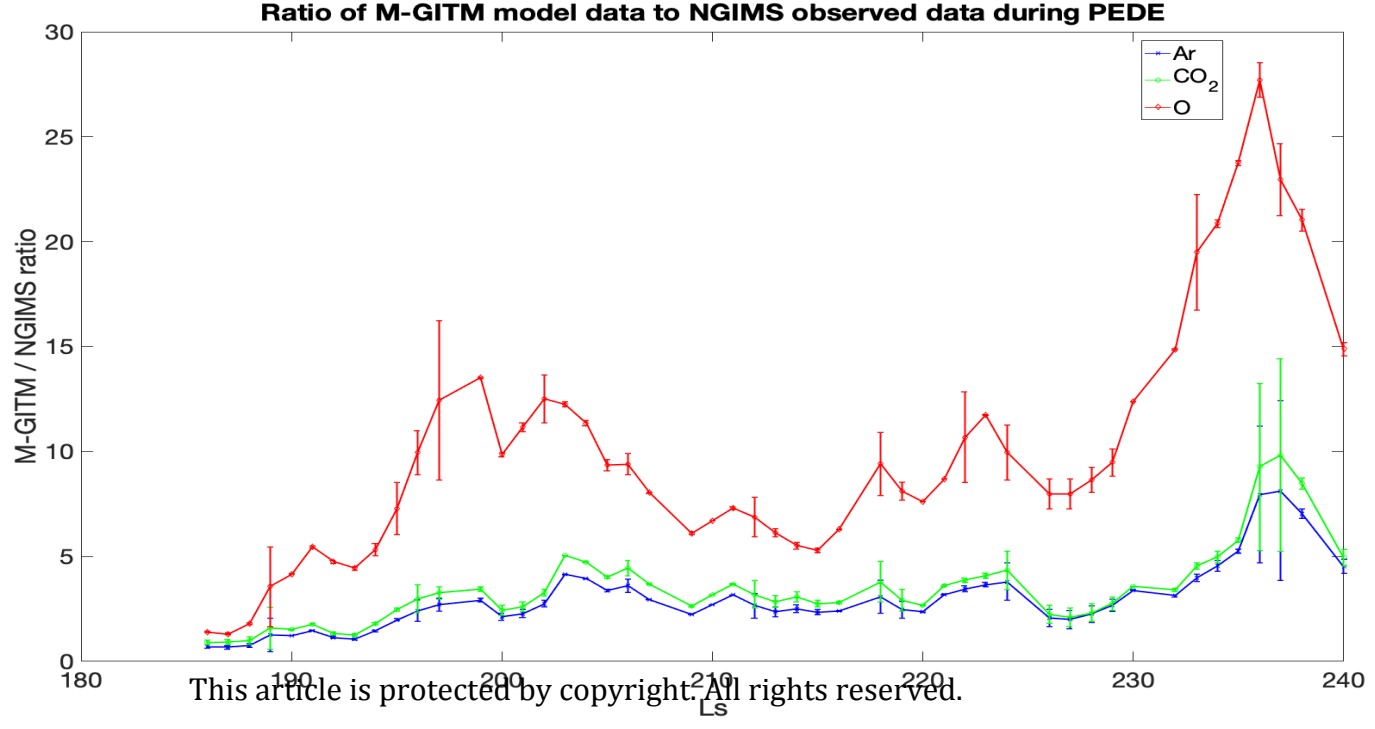

(b)